A Sox2:miR-486-5p Axis Regulates Survival of GBM Cells by Inhibiting Tumor Suppressor Networks

Hernando Lopez-Bertoni[1,2], Ivan S. Kotchetkov[3], Nicole Mihelson[4], Bachchu Lal[1,2], Yuan Rui[5], Heather Ames[6], Maria Lugo-Fagundo[1], Hugo Guerrero-Cazares[7,8], Alfredo Quiñones-Hinojosa[7,8], Jordan J. Green[5,7,9,10,11], and John Laterra[1,2,10,12]

ABSTRACT

Glioblastoma multiforme (GBM) and other solid malignancies are heterogeneous and contain subpopulations of tumor cells that exhibit stem-like features. Our recent findings point to a dedifferentiation mechanism by which reprogramming transcription factors Oct4 and Sox2 drive the stem-like phenotype in glioblastoma, in part, by differentially regulating subsets of miRNAs. Currently, the molecular mechanisms by which reprogramming transcription factors and miRNAs coordinate cancer stem cell tumor-propagating capacity are unclear. In this study, we identified miR-486-5p as a Sox2-induced miRNA that targets the tumor suppressor genes *PTEN* and *FoxO1* and regulates the GBM stem-like cells. miR-486-5p associated with the GBM stem cell phenotype and Sox2 expression and was directly induced by Sox2 in glioma cell lines and patient-derived neurospheres. Forced expression of miR-486-5p enhanced the self-renewal capacity of GBM neurospheres, and inhibition of endogenous miR-486-5p activated PTEN and FoxO1 and induced cell death by upregulating proapoptotic protein BIM via a PTEN-dependent mechanism. Furthermore, delivery of miR-486-5p antagomirs to preestablished orthotopic GBM neurosphere-derived xenografts using advanced nanoparticle formulations reduced tumor sizes *in vivo* and enhanced the cytotoxic response to ionizing radiation. These results define a previously unrecognized and therapeutically targetable Sox2:miR-486-5p axis that enhances the survival of GBM stem cells by repressing tumor suppressor pathways.

Significance: This study identifies a novel axis that links core transcriptional drivers of cancer cell stemness to miR-486-5p–dependent modulation of tumor suppressor genes that feeds back to regulate glioma stem cell survival.

Introduction

Neoplastic cells are inherently plastic and reprogramming transcription factors (e.g., Oct4 and Sox2) are commonly overexpressed in cancer and play critical roles in tumor cell fate determination through the process of reprogramming (1). Brain tumors are among the most devastating forms of cancer and glioblastoma (GBM) represents the most aggressive and lethal form of the disease (2). GBM is characterized by small subsets of cells, referred to as glioma stem cells (GSC), which display stem-like properties including unlimited self-renewal and multilineage differentiation (3). These stem-like cells act as critical determinants of GBM resistance to current treatments and are thought to play an important role in tumor recurrence (4). Approaches aimed at targeting mechanisms of GBM cell self-renewal and therapeutic resistance hold great potential for the development of novel therapeutics to treat GBM (4).

Members of the *SOX* family of transcription factors are potent drivers of somatic cell reprogramming and dysregulation of its members has been implicated in several disease conditions including cancer (5). The *SOXB1* subclass, composed of Sox1, 2, and 3, functions to establish and maintain a stem-like state in embryonic stem cells and neural progenitor cells (6). Of these three transcription factors, Sox2 is sufficient to induce cell reprogramming in multiple contexts making it a potent regulator of the stem cell phenotype (7). Sox2 dysregulation alters networks of coding and noncoding genes that affect migration, invasion, growth, survival, and self-renewal capacity of multiple tumor cell types, including GBM (5). *SOX2* gene expression is upregulated in glioma compared with normal brain and silencing of Sox2 results in loss of tumor-propagating capacity of GBM stem-like cells (8, 9). How stemness-enhancing mechanisms regulated by Sox2 affect the genetic and epigenetic landscape of GBM stem-like cells and which of these changes are amenable to therapeutic intervention remain unclear (5).

Growing evidence highlight miRNAs as key determinants of cell fate and tumorigenesis (10). These short noncoding RNAs are negative regulators of gene expression that are often dysregulated in cancer with the capacity to act as oncogenes or tumor suppressors (10). Not surprisingly, dedifferentiating events driven by reprogramming transcription factors modify noncoding RNA networks and Sox2 has been shown to drive these changes in GBM stem-like cells (11, 12). We

[1]Hugo W. Moser Research Institute at Kennedy Krieger, Baltimore, Maryland. [2]Department of Neurology, Johns Hopkins University School of Medicine, Baltimore, Maryland. [3]Department of Neurology, Memorial Sloan Kettering Cancer Center, New York, New York. [4]National Institute of Neurological Disorders and Stroke, NIH, Bethesda, Maryland. [5]Department of Biomedical Engineering, Institute for NanoBioTechnology, and the Translational Tissue Engineering Center, Johns Hopkins University School of Medicine, Baltimore, Maryland. [6]Department of Pathology, University of Maryland School of Medicine, Baltimore, Maryland. [7]Department of Neurosurgery, Johns Hopkins University School of Medicine, Baltimore, Maryland. [8]Department of Neurosurgery, Mayo Clinic, Jacksonville, Florida. [9]Department of Ophthalmology, Johns Hopkins University School of Medicine, Baltimore, Maryland. [10]Department of Oncology, Johns Hopkins University School of Medicine, Baltimore, Maryland. [11]Departments of Materials Science & Engineering and Chemical & Biomolecular Engineering, Johns Hopkins University, Baltimore, Maryland. [12]Department of Neuroscience, Johns Hopkins University School of Medicine, Baltimore, Maryland.

Note: Supplementary data for this article are available at Cancer Research Online (http://cancerres.aacrjournals.org/).

Corresponding Authors: John Laterra, The Johns Hopkins School of Medicine, 707 N. Broadway, Baltimore, MD 21205. Phone: 443-923-2679; Fax: 443-923-2695; E-mail: Laterra@kennedykrieger.org; and Hernando Lopez-Bertoni, Hugo W. Moser Research Institute at Kennedy Krieger, 707 North Broadway, Baltimore, MD 21205. E-mail: Lopezbertoni@kennedykrieger.org

Cancer Res 2020;80:1644–55

doi: 10.1158/0008-5472.CAN-19-1624

recently uncovered a novel molecular circuit by which Oct4 and Sox2 coexpression induces glioma cell stemness and tumor-propagating capacity by altering DNA methylation and modifying miRNA networks (13). We previously demonstrated that Oct4/Sox2 coexpression induces DNA methylation events that repress stemness-inhibiting miRNAs and that reconstituting these miRNAs potently inhibits GBM cell stemness and tumor growth *in vivo* (14, 15).

The goal of this study is to elucidate how miRNA subsets that are upregulated by reprogramming transcription factors regulate GBM-propagating stem cells and glioma growth. We present the novel findings that miR-486-5p, an miRNA not previously known to regulate GBM neurospheres, is induced by Sox2 under conditions that promote GBM cell stemness. Exogenous expression of miR-486-5p or Sox2 repressed tumor suppressor genes *PTEN* and *FoxO1* and transgenic miR-486-5p enhanced resistance of GBM neurosphere cells to ionizing radiation (IR) treatment. In addition, we show that PTEN is the dominant target through which miR-486-5p regulates neurosphere cell survival and that inhibiting miR-486-5p impedes the growth and enhances the radiosensitivity of established GBM xenografts. These findings demonstrate that Sox2 controls GBM cell survival by activating miR-486-5p that inhibits tumor suppressor networks and identifies miR-486-5p inhibition as a potential strategy for treating GBM.

Materials and Methods

GBM neurosphere culture

GBM-derived neurosphere lines (GBM1A and GBM1B) were originally derived and characterized by Vescovi and colleagues (16). The GBM-KK neurosphere line was derived from a single GBM patient and kindly provided by Dr. Jaroslaw Maciaczyk (University of Freiburg, Freiburg, Germany). Low-passage primary neurospheres were derived directly from human GBM clinical specimens and from patient-derived xenografts obtained from pathologic GBM specimens obtained during clinically indicated surgeries at Johns Hopkins Hospital (Baltimore, MD) using established methods (5). The human GBM xenograft line, Mayo39, was originally obtained from the Mayo Clinic (17). All neurospheres were cultured in serum-free medium containing DMEM/F-12 (Invitrogen), supplemented with 1% BSA, 20 ng/mL EGF, and 10 ng/mL fibroblast growth factor (FGF).

The human embryonic kidney 293FT (HEK293FT) cell line was obtained from the ATCC and was maintained in Dulbecco's modified Eagle/F12 medium (1:1, vol/vol) supplemented with 10% FBS (Thermo Fisher Scientific Inc). The 293FT cells were grown at 37°C in a humidified incubator with 5% CO_2. All cell lines used in the study were tested for *Mycoplasma* and were short tandem repeat profiled. All experiments using transgenic cells were performed within 10 passages of generating the cells lines.

Intracranial nano-miR delivery and tumor formation *in vivo*

A transcranial cannula was placed so that the tip is in the right caudate/putamen of female athymic nude NCR Nu/Nu mice (8-week-old). One week after cannula placement, animals received 1.0×10^4 GBM1A or Mayo39 tumor-propagating cells via the cannula and assigned into different treatment groups in a nonblinded, randomized manner. Using the same cannula, the control cohort received nano-miRs loaded with control miRNA labeled with Dy547 and the experimental group received nano-miRs loaded with the miR-486-5p inhibitor.

Stainless steel guide and dummy cannulas were custom ordered from PlasticsOne. The guide cannula (26 gauge) was designed to have a Decon mesh under the pedestal and cut 3 mm from the mesh. The guide cannula is capped with a screw-on dummy cannula 6.5 mm long so that a 0.5 mm projection extends past the guide to prevent blockage. Prior to surgical placement of cannulas, mice were anesthetized using a ketamine (100 mg/Kg)/xylazine (10 mg/kg) cocktail and mounted on a stereotactic frame. A rostro-caudal incision was made with a scalpel, the skin is spread apart, the surface of the skull was exposed, and cannulas were placed at coordinates: AP (antero-posterior) 0.0 (0 mm from bregma), L (lateral) 1.8 (1.8 mm right from mid-sagittal line).

Lyophilized and resuspended nano-miRs were slowly infused (5 μL) into the brains (0.5 μL/minute with a 2-minute wait at the end) twice a week as described for each experiment. At the end of the experiment, animals were anesthetized and then sacrificed by perfusion using 4% paraformaldehyde (PFA) according to methods approved by the Animal Use and Care Committee at Johns Hopkins University (Baltimore, MD). All the sectioning and histologic analysis was performed in-house. Whole brains were collected and soaked in 4% PFA for 2 days then washed 1× with PBS and soaked in 30% sucrose overnight at 4°C then flash frozen using dry ice. Brains were embedded in Tissue-Tek O. C.T. Compound (VWR) and 20-μm sections were cut using the CryoStat system from Microm. All tumor sections were analyzed by a neuropahologist in a blinded fashion.

For ionizing radiation experiments, a subset of animals received radiation either alone or in combination with the nano-miR therapy. Radiation was administered starting 8 weeks after tumor cell implantation. Tumor-bearing mice were gently restrained in a 50 mL ventilated plastic centrifuge tube encapsulated in lead cylinders to protect normal body parts from radiation. This ensures only the tumor-bearing brain will be irradiated. Animals received 300 cGy (or sham irradiation) once a week for 2 weeks using a collimator ^{137}Cs source. These radiation doses were without adverse side effects.

Tumor growth inhibition was determined by computer-assisted morphometric quantification of tumor area in hematoxylin and eosin–stained histologic sections using ImageJ software and volumes calculated using volume = (square root of maximum cross-sectional area)^3. Data for all *in vivo* experiments are shown as the mean tumor area distribution of all animals used in the study. All animal procedures were approved by the Johns Hopkins Institutional Animal Care and Use Committee (protocol # MO14M307), and were in accordance with the NIH Guide for the Care and Use of Laboratory Animals.

Tumor sections were analyzed by a neuropathologist (H. Ames) for histologic features of GBM including necrosis. To measure necrosis, the total areas of viable tumor and necrosis within each tumor were identified by an expert neuropathologist and quantified using ImageJ software from images taken at 10× magnification and represented as (area of necrotic tissue/area of total tumor tissue) × 100.

Statistical analysis

All experiments were performed in triplicates and repeated at least twice in each cell model ($N \geq 6$). PRISM GraphPad 7 was used to perform all the statistical analyses presented. Two-group comparisons were analyzed for variation and significance using a two-tailed, type I *t* test and *P* values lower than 0.05 were considered significant and symbolized by an asterisk in the graphs. One-way or two-way ANOVA and Tukey *post hoc* test was used to analyze the relationships when comparing multiple variables, with *P* values lower than 0.05 considered to be statistically significant. All data shown are representative of means ± SD of triplicate results unless otherwise specified.

Additional information about polymer synthesis, primers used for qRT-PCR (Supplementary Tables S1–S3), cloning (Supplementary Table S4), lentiviral constructs (Supplementary Table S5), antibodies

(Supplementary Table S6), and miRNA array results (Supplementary Table S7) can be found in the Supplementary Materials.

Results

miR-486-5p associates with the GBM stem cell phenotype and is induced by Sox2

Our previously published miRNA-array screen uncovered 10 candidate miRNAs upregulated (≥2-fold) in human GBM–derived neurospheres following Oct4 and Sox2 coexpression (13). We confirmed by qRT-PCR that Oct4/Sox2 activates the expression of a subset of those precursor (pre-) miRNAs (i.e., miR-23a, miR-10b, miR-138, miR-222, and miR-486-5p; **Fig. 1A**). We next examined multiple endpoints to determine whether these miRNAs associate with GBM cell stemness. Forced differentiation of GBM neurospheres, a condition that also inhibits Oct4 and Sox2 expression (13), decreased levels of pre-miR-23a, pre-miR-138, and pre-miR-486-5p in multiple neurosphere lines (**Fig. 1B**). $CD133^+$ and SSEA-1^+ cell subpopulations enriched for stem-like cells expressed 2- to 3-fold higher levels of both pre-miR-23a and pre-miR-486-5p compared with the $CD133^-$ or $SSEA^-$ cells. We found no significant differential expression of pre-miR-138 in $SSEA^+$ or $CD133^+$ cells (**Fig. 1C**).

These associations led us to hypothesize that miR-23a and miR-486-5p act to support the GBM stem-like phenotype, a function consistent with their induction by Oct4/Sox2 expression, upregulation in $SSEA^+$ and $CD133^+$ cells, and repression in response to forced differentiation (13). To test this hypothesis, we forced the expression these miRNAs individually using lentiviral expression vectors and measured effects on sphere-forming capacity as a surrogate for stem cell self-renewal (Supplementary Fig. S1). qRT-PCR analysis following lentivirus transduction demonstrated 10- to 18-fold increase in mature miR-23a, miR-138, and miR-486-5p expression. Only miR-486-5p had the capacity to enhance sphere-forming capacity (Supplementary Fig. S1). To directly evaluate the effects of miR-486-5p on the GBM stem cell phenotype, three patient-derived neurosphere lines were transduced using lentivirus expressing miR-486-5p precursor miRNA and sphere-forming capacity was determined by limiting dilution assay, a quantitative marker of cell stemness and self-renewal. Cells

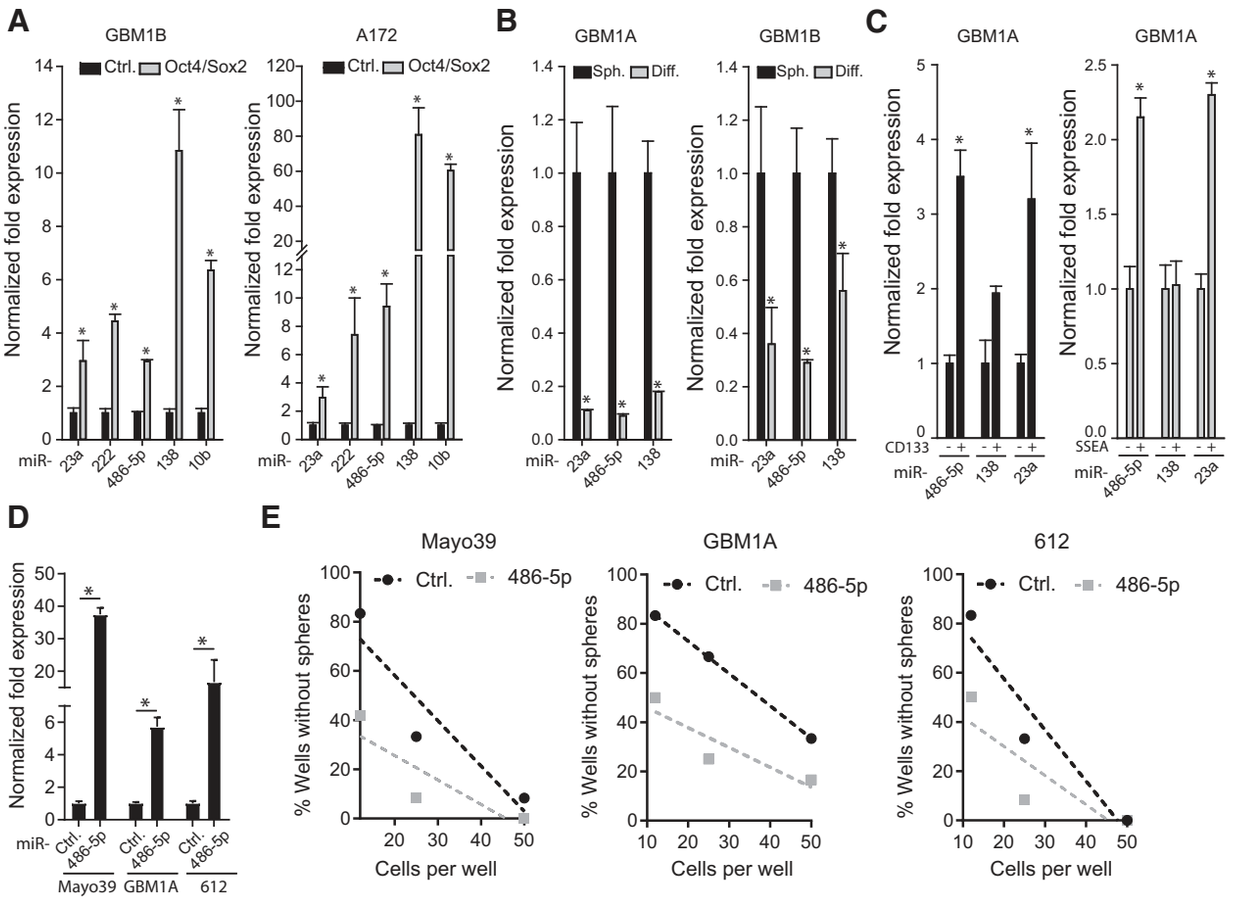

Figure 1.

miR-486-5p associates with the GBM stem cell phenotype. **A,** qRT-PCR to measure effects of Oct4/Sox2 coexpression on a subset of miRNAs detected by PCR array (13) to be upregulated in GBM neurospheres. **B,** qRT-PCR analysis showed decreased expression of pre-miR-23a, pre-miR-486-5p, and pre-miR-138 5 days after forced differentiation of GBM neurospheres. **C,** GBM neurosphere cells expressing stem cell markers CD133 or SSEA were separated into marker-positive and marker-negative populations by flow cytometry. qRT-PCR was used to measure expression of selected pre-miRNAs in the different cell subsets. **D,** qRT-PCR analysis to measure expression of mature miR-486-5p in three different GBM neurosphere isolates. **E,** Limiting dilution assay in neurosphere isolates transduced with a control lentivirus or a lentivirus expressing miR-486-5p. Statistical significance was calculated using Student *t* test in **A–D** and data are presented as means ± SD. *, $P < 0.05$.

transduced with a scrambled miRNA were used as a negative control. Forced expression of miR-486-5p enhanced self-renewal capacity of all three patient-derived neurosphere lines tested (**Fig. 1D** and **E**). These results show that Oct4/Sox2 coexpression activates a subset of miRNAs that correlate with the stem-like phenotype of GBM cells and predicts that miR-486-5p functions to regulate GBM cell growth patterns.

Comparative PCR array data examining changes in miRNA levels in response to expression of either exogenous Oct4 or Sox2 in neurosphere cells suggests that miR-486-5p is preferentially induced by Sox2

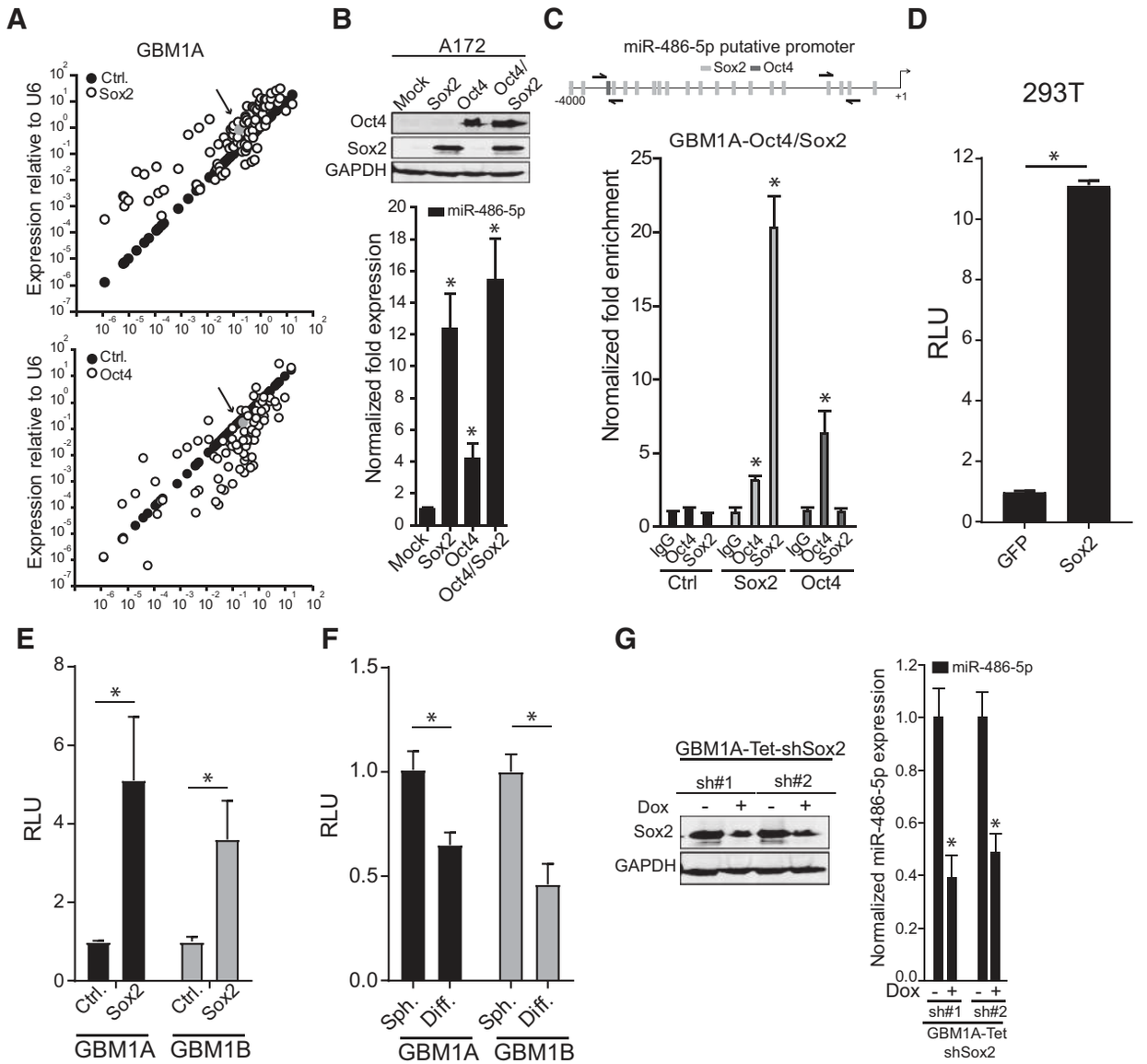

Figure 2.

miR-486-5p is regulated by SOX2. **A,** Differential miRNA expression was determined in GBM1A neurospheres expressing Oct4 or Sox2 relative to control GBM1A spheres using a human brain cancer miRNA PCR array. Arrow, gray dot indicating miR-486-5p expression. **B,** Top, Western blot analysis showing relative expression of Sox2 and Oct4. Bottom, qRT-PCR to measure expression of mature miR-486-5p 3 days after exogenous expression of Oct4, Sox2, or the combination. **C,** Top, Oct4 and Sox2 binding sites on human miR-486-5p promoter. Arrows, primer sites used for PCR analyses. Bottom, DNA purified from chromatin immunoprecipitation was analyzed by qRT-PCR using primer pairs designed to amplify fragments containing Oct4, Sox2, or a control region lacking binding sites for either transcription factor. **D,** 293T cells were cotransfected with a luciferase reporter construct spanning the miR-486-5p putative promoter containing the SOX2-binding sites and GFP or SOX2. **E,** GBM neurosphere isolates expressing exogenous SOX2 were transfected with the luciferase reporter construct spanning the miR-486-5p putative promoter containing the SOX2-binding sites and luciferase activity was measured 3 days after transfection. **F,** GBM1A and GBM1B neurospheres were transfected with luciferase reporter construct covering the miR-486-5p putative promoter containing the SOX2 binding and forced to differentiate. Luciferase activity was measured 3 days after differentiation. **G,** Western blot analysis to measure expression of Sox2 (top) and qRT-PCR to measure expression of pre-miR-486-5p (bottom) 3 days after doxycycline treatment. Student *t* test was used to calculate statistical significance in **D**–**G**; one-way ANOVA with Tukey *post hoc* test was used calculate statistical significance in **B** and **C**. Data are presented as means ± SD. *, $P < 0.05$.

alone (**Fig. 2A**; Supplementary Table S7). To confirm this prediction, we expressed transgenic Oct4, Sox2, or their combination in A172 GBM cells, which have very low expression of endogenous Oct4 and Sox2, and measured expression of mature miR-486-5p using qRT-PCR. Exogenous Sox2, Oct4, or their combination induced mature miR-486-5p expression by 12-, 4-, and 15-fold, respectively (**Fig. 2B**). *In silico* analysis shows enrichment for Sox2-binding sites in the putative promoter region 5′ from the miR-486-5p transcription start site (**Fig. 2C**, top), suggesting Sox2 directly transactivates miR-486-5p gene expression in.

Quantitative chromatin immunoprecipitation (ChIP) supports this prediction by showing approximately 20-fold enrichment of Sox2 binding compared with an approximately 6-fold enrichment of Oct4 binding at the predicted promoter sites (**Fig. 2C**, bottom). Promoter–reporter assays were used to determine whether Sox2 transactivates this region of the miR-486-5p promoter. The region of the human miR-486-5p promoter containing the Sox2-binding site identified in our ChIP experiments (**Fig. 2C**) was cloned into a luciferase reporter cassette and cotransfected into HEK293T in the presence of Sox2 or GFP. Compared with control cells transfected with GFP, Sox2 induced miR-486-5p/luciferase activity approximately 11-fold (**Fig. 2D**). A similar increase was observed when this same luciferase reporter plasmid was transfected into GBM1A and GBM1B neurospheres stably expressing transgenic Sox2 (**Fig. 2E**). Using a similar approach, we measured a 40%–50% decrease in luciferase activity from the miR-486-5p luciferase reporter when we forced neurosphere cells to differentiate (**Fig. 2F**), a condition that decreases endogenous expression of Sox2. To test whether Sox2 is required to maintain expression of endogenous miR-486-5p, we generated transgenic neurospheres lines expressing shRNA hairpins specific for Sox2 under the control of a doxycyline-induced promoter (Tet-shSox2). shRNA-mediated knockdown of Sox2 decreased expression of pre-miR-486-5p by 50%–60% (**Fig. 2G**). Taken together, these results show that Sox2 plays a significant role in driving miR-486-5p expression.

The Sox2:miR-486-5p axis inhibits tumor suppressor gene expression

miRNAs function as negative regulators of gene expression and their function is determined by the genes and networks they modulate (18). Combining miR-486-5p targets predicted by 3 different

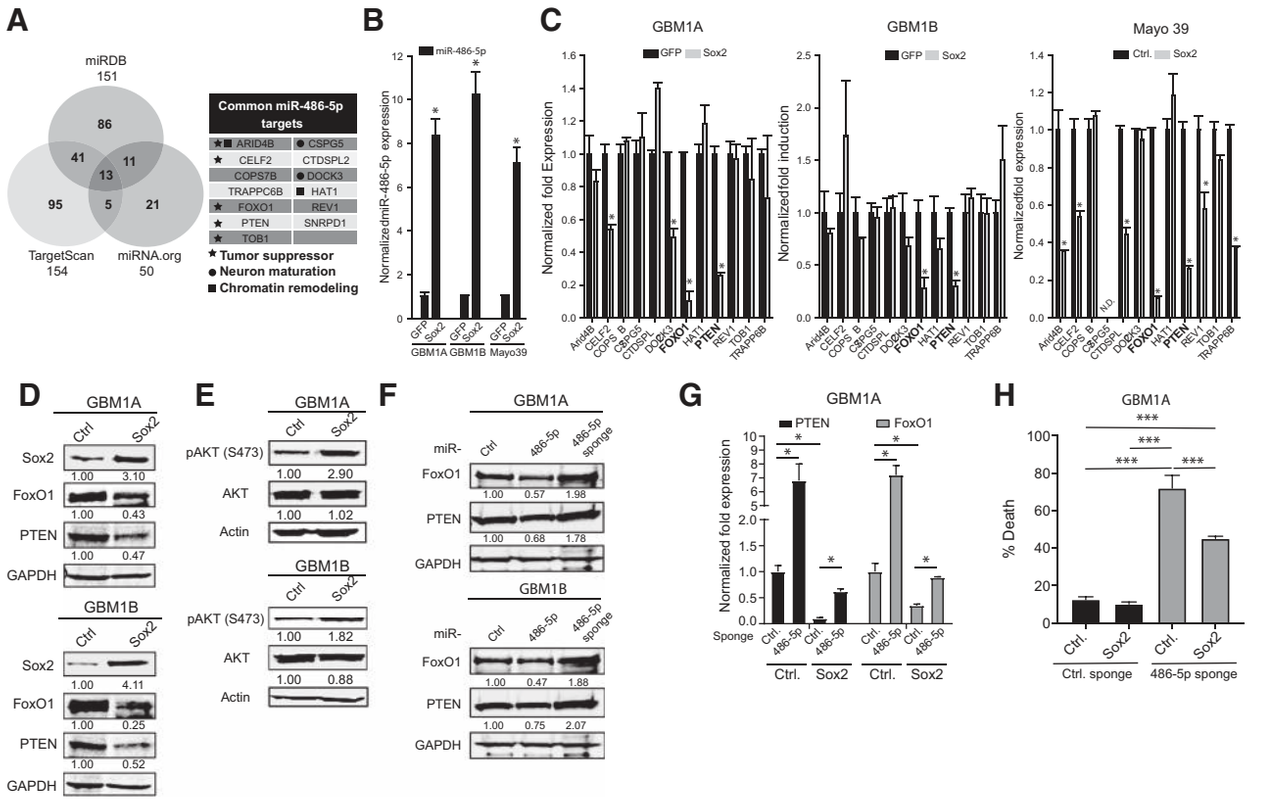

Figure 3.

Sox2:miR-486-5p axis downregulates tumor suppressor genes in GBM neurospheres. **A,** Left, Venn diagram showing intersection of miR-486-5p target genes using three different prediction algorithms. Right, list of high-confidence miR-486-5p target genes. **B,** qRT-PCR to measure expression of mature miR-486-5p in GBM neurosphere cells expressing transgenic Sox2. **C,** qRT-PCR to measure gene levels of high-confidence miR-486-5p target genes in GBM neurospheres expressing transgenic Sox2. Genes highlighted in bold (*FOXOI, PTEN*) were commonly regulated in three distinct GBM neurosphere isolates. **D,** Western blot analysis to measure PTEN and FoxO1 protein levels in GBM neurospheres expressing transgenic Sox2. **E,** Western blot analysis to measure AKT and pAKT protein levels in GBM neurospheres expressing transgenic Sox2. **F,** Western blot analysis to measure PTEN and FoxO1 protein levels in GBM neurospheres 4 days after expressing transgenic miR-486-5p or miR-486-5p inhibition (miR-486-5p sponge). **G,** qRT-PCR to measure PTEN and FoxO1 expression in GBM neurospheres expressing transgenic SOX2 after miR-486-5p inhibition. **H,** Trypan blue exclusion to measure cell death 4 days after miR-486-5p inhibition in in GBM neurospheres expressing transgenic SOX2. Student *t* test was used to calculate statistical significance in **B** and **C**; one-way ANOVA with Tukey *post hoc* test was used calculate statistical significance in **H**. Data are presented as means ± SD. *, $P < 0.05$; ***, $P < 0.001$.

bioinformatics algorithms generated a list of high-confidence gene candidates potentially regulated by the Sox2:miR-486-5p axis in GBM neurospheres (**Fig. 3A**). We screened neurosphere cells expressing miR-486-5p induced by exogenous Sox2 (**Fig. 3B**) to identify which of the 13 candidate target genes were likely to function downstream of miR-486-5p. PTEN and FoxO1 were the only candidate targets consistently downregulated by exogenous Sox2 in multiple GBM cell models (**Fig. 3C**). Downregulation of PTEN and FoxO1 by forced Sox2 expression was confirmed using Western blot analysis (**Fig. 3D**; Supplementary Fig. S2A). PTEN inhibits the activation (i.e., phosphorylation) of Akt, a tumor promoter that regulates FoxO1 (19). Forced expression of either Sox2 or miR-486-5p increased Akt phosphorylation (pAKT), consistent with the downregulation of PTEN (**Fig. 3E**; Supplementary Fig. S2B). The seed region for miR-486-5p is highly conserved among several species in the PTEN and FoxO1 3′UTR (Supplementary Fig. S2C) consistent with their direct targeting by miR-486-5p and functional significance. As predicted, we observed a significant decrease in PTEN and FoxO1 protein and mRNA in response to exogenous miR-486-5p (**Fig. 3F**; Supplementary Fig. S2D). Neurospheres were transduced with lentivirus expressing miRNA sponges against miR-486-5p to test whether endogenous miR-486-5p regulates PTEN and/or FoxO1 expression. Control lentivirus expressing a scrambled sequence was used a negative control. miR-486-5p inhibition increased levels of PTEN and FoxO1 in neurosphere lines and primary cells derived from a patient-derived GBM xenograft (**Fig. 3G**; Supplementary Fig. S2E). We also observed that inhibiting miR-486-5p partially rescued the repression of PTEN and FOXO1 by exogenous Sox2 (**Fig. 3H**). Reexpression of PTEN and FOXO1 via miR-486-5p inhibition induced cell death even in the presence of exogenous Sox2, consistent with miR-486-5p functioning as a downstream effector of Sox2. Taken together, these results demonstrate that Sox2 inhibits PTEN and FoxO1 tumor suppressor pathways by directly inducing miR-486-5p as an intermediate.

Gene expression profiles from surgical specimens were used to explore the broader potential clinical relevance of the Sox2:miR-486-5p axis. Analysis of The Cancer Genome Atlas (TCGA) datasets (HG-U133A) reveals high miR-486-5p expression levels in GBM compared with normal brain (**Fig. 4A**). This same relationship persists in each GBM subtype relative to normal brain (**Fig. 4B**). In addition, miR-486-5p expression was found to be upregulated in a panel of 18 independently isolated primary human GBM-derived neurosphere isolates compared with cells derived from normal human brain (**Fig. 4C**). Further analysis of these primary neurosphere isolates revealed a significant positive correlation between Sox2 and

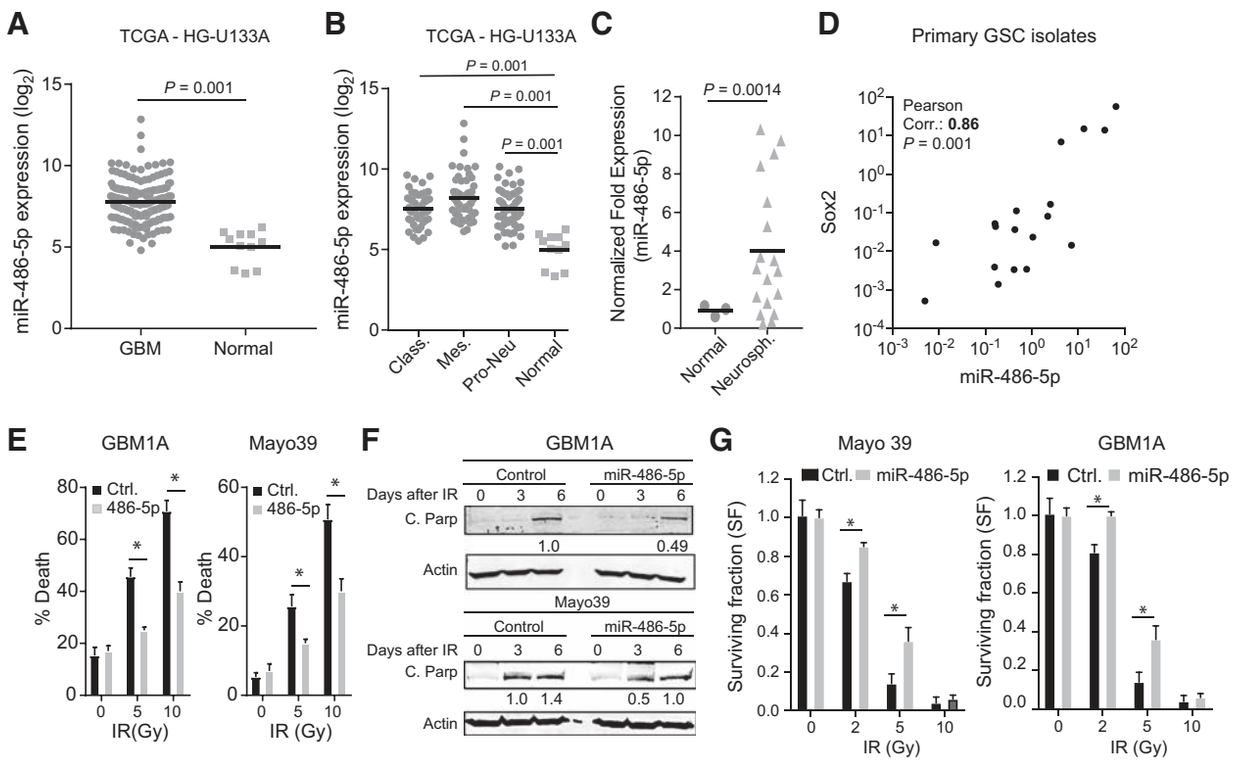

Figure 4.

miR-486-5p is upregulated in GBM and enhances resistance to IR treatment. miR-486-5p expression data was retrieved from the TCGA database using the BETASTASIS portal (http://www.betastasis.com). **A** and **B,** miR-486-5p levels in normal brain compared with all GBM (**A**) or compared with GBM subtypes (**B**). **C,** qRT-PCR to measure miR-486-5p expression in GBM neurospheres lines and primary GBM neurosphere isolates compared with nontumorigenic glial progenitors (normal). **D,** Positive correlation between miR-486-5p and Sox2 expression in primary GBM neurosphere isolates. Pearson coefficient analysis was applied to establish correlations from gene expression data. **E,** GBM stem-like cells stably expressing miR-486-5p or a control miRNA (Ctrl.) were treated with increasing doses of IR and cell death was quantified using Trypan blue exclusion 3 days after treatment. **F,** Western blot to measure cleaved PARP in GBM stem-like cells expressing transgenic miR-486-5p 3 and 6 days after IR (5 Gy) treatment. **G,** Clonogenic assay in GBM stem-like cells expressing transgenic miR-486-5p after IR treatment. Colonies were counted using ImageJ script 14 days after treatment. Student *t* test was used to calculate statistical significance in **B–D**; two-way ANOVA with Tukey *post hoc* test was used calculate statistical significance in **E** and **G**. Data are presented as means ± SD. *, $P < 0.05$.

miR-486-5p expression (**Fig. 4D**). Thus, miR-486-5p expression was increased in GBM neurospheres, $CD133^+$, and $SSEA^+$ subsets, and directly correlated with Sox2 expression. We also observe a significant negative correlation between Sox2 and PTEN or FoxO1 expression in these clinical datasets (Supplementary Fig. S3). These observations are further supported by the negative correlation measured between Sox2 and FoxO1 expression in low-passage primary human neurospheres derived directly from human GBM surgical specimens (Supplementary Fig. S3) consistent with our findings that Sox2 downregulates PTEN and FoxO1 *in vitro*. Together, these results are consistent with PTEN and FoxO1 being downstream of a Sox2:miR-486-5p axis in GBM.

miR-486-5p regulates GBM cell survival

Our results showing that miR-486-5p inhibits tumor suppressor pathways (**Fig. 2**) coupled with the clinical associations lead us to hypothesize that miR-486-5p induces glioma resistance to DNA-damaging agents. To test this hypothesis, we examined the effect of exogenous miR-486-5p on the GBM neurosphere response to ionizing radiation (IR). Cells expressing exogenous miR-486-5p were more resistant to death induced by either 5 Gy or 10 Gy IR as determined by Trypan blue exclusion assay (**Fig. 4E**). The cytoprotective activity of miR-486-5p was further supported by Western blot analysis showing lower levels of cleaved PARP, a well described marker of apoptosis (**Fig. 4F**). Clonogenic assay for long-term cell survival also showed that exogenous miR-486-5p protects GBM neurospheres from 2 Gy and 5 Gy radiation toxicity, but not 10 Gy (**Fig. 4G**).

To test the hypothesis that endogenous miR-486-5p functions as a prosurvival factor, GBM-derived neurospheres were transduced with lentivirus expressing either a scrambled RNA sequence or an antisense RNA oligo designed to inhibit miR-486-5p (miR-486-5p sponge). The miR-486-5p sponge efficiently decreased the levels of endogenous pre-miR-486-5p in multiple independent GBM-derived cell models by >80%, as measured by qRT-PCR (Supplementary Fig. S4). Inhibition of endogenous miR-486-5p triggered apoptosis in these cells as evidenced by an increase in dead cells measured by Trypan blue exclusion and caspase-3 cleavage (**Fig. 5A** and **B**).

To further dissect the mechanism of cell death induced by miR-486-5p inhibition, we measured expression of multiple members of the

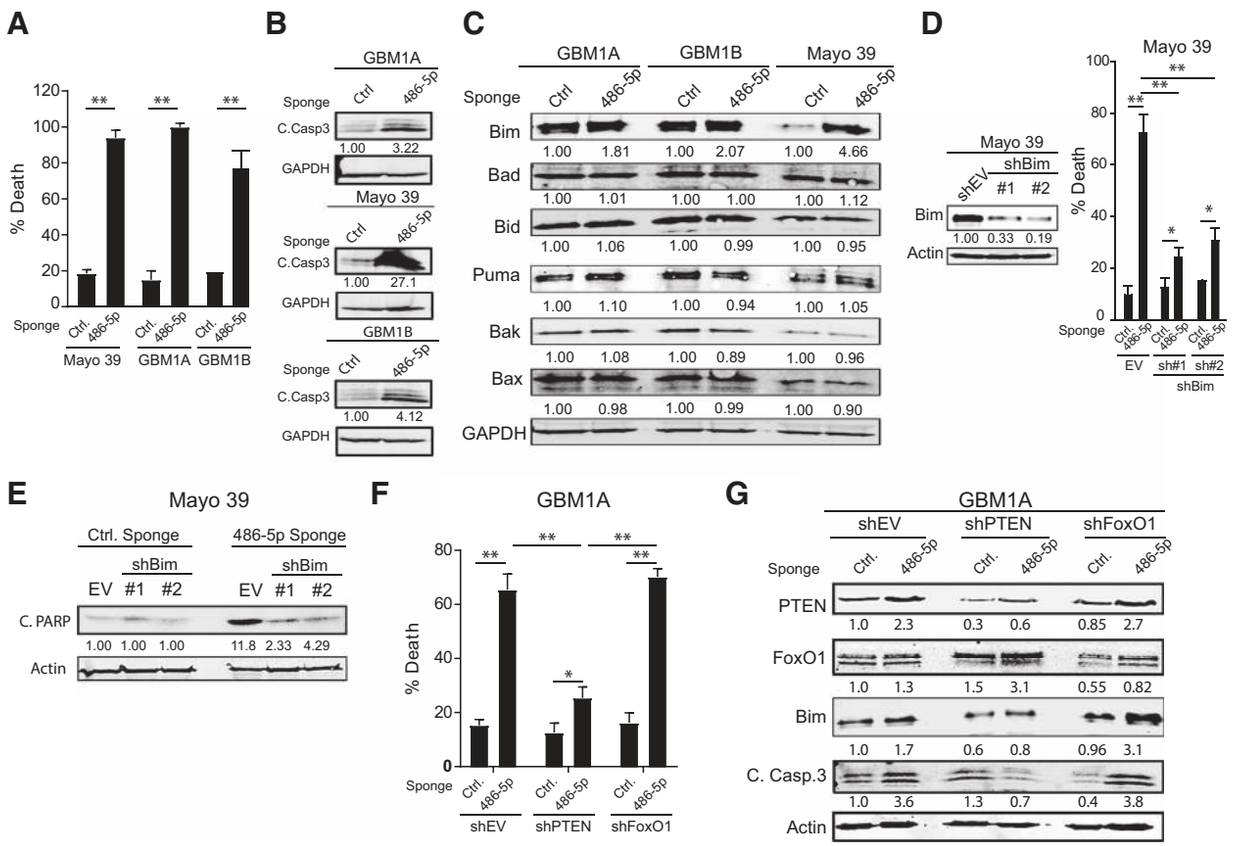

Figure 5.

miR-486-5p inhibition activates Bim and induces apoptosis in GBM neurospheres. **A,** Equal numbers of GBM1A neurosphere cells transduced with lentiviral constructs expressing a miR-486-5p sponge or a control vector were cultured in neurosphere medium containing EGF/FGF for 14 days and neurosphere numbers (>100 μm diameter) were quantified by computer-assisted image analysis. **B,** Western blot analysis showing cleaved caspase-3 6 days after miR-486-5p inhibition. **C,** Western blots showing expression of proapoptotic proteins 3 days after miR-486-5p inhibition. **D,** Mayo 39 primary GBM cells were transduced with two independent shRNA hairpins targeting BIM. Left, Western blot analysis showing BIM levels following shRNA knockdown. Right, cell viability 5 days after miR-485-5p inhibition in cells transduced with shEV or shBim. **E,** Western blot showing PARP cleavage 5 days after miR-485-5p inhibition in cells transduced with shEV or shBim. **F,** Cell viability 5 days after miR-485-5p inhibition in cells transduced with shEV, shPTEN, or shFoxO1. **G,** Western blot analysis showing expression of PTEN, FoxO1, Bim, and cleaved caspase-3 in GBM1A neurospheres after PTEN or FoxO1 knockdown and miR-486-5p inhibition. Student *t* test was used to calculate statistical significance in **A**; two-way ANOVA with Tukey *post hoc* test was used calculate statistical significance in **D** and **F**. Data are presented as means ± SD. *, $P < 0.05$; **, $P < 0.01$.

Bcl-2 family of proteins that are critical regulators of cell survival (20). Western blot analysis revealed a consistent increase in the BH3-only protein Bim following miR-486-5p inhibition in multiple GBM neurosphere lines (**Fig. 5C**). Bim is a potent initiator of apoptosis shown to be sufficient to induce cell death in multiple settings (21). To test whether Bim upregulation is responsible for the cell death effects observed after miR-486-5p inhibition, we knocked-down endogenous Bim using two independent shRNA hairpins (**Fig. 5D**, left) and then inhibited miR-486-5p as described above. An empty vector (shEV) was used as negative control for shBim. Bim repression rescued cells from the death induced by miR-486-5p inhibition by approximately 75% as measured by Trypan blue exclusion assay (**Fig. 5D**, right) and Western blot analysis of PARP cleavage (**Fig. 5E**).

Both PTEN and FoxO1 have been shown to regulate proapoptotic BH3-only protein Bim (22). To determine whether either PTEN or FoxO1 plays a dominant role in the capacity of miR-486-5p to regulate Bim and downstream apoptotic death, we examined how PTEN or FoxO1 knockdown affects the response to miR-486-5p inhibition. As before, an empty vector (shEV) was used as negative control. PTEN knockdown was sufficient to impair Bim induction and cell killing in response to miR-486-5p inhibition. In contrast, FoxO1 knockdown had no effect (**Fig. 5F** and **G**). These observations were confirmed using a second shRNA targeting PTEN (Supplementary Fig. S5). Together, these results identify miR-486-5p as a critical determinant of cell survival and identify PTEN as the principal functional downstream effector by which miR-486-5p inhibition induces Bim and apoptosis.

Suppression of miR-486-5p *in vivo* inhibits growth of orthotopic GBM xenograft and sensitizes xenografts to IR treatment

Our *in vitro* findings predict that *in vivo* inhibition of miR-486-5p will hinder tumor growth and potentially cooperate with cytotoxic therapeutics. As a first step to evaluate this using a clinically translatable miRNA delivery platform, bioreducible nanoparticles (15) containing a scrambled miRNA sequence or the miR-486-5p sponge were used to transfect GBM neurospheres and primary cells from patient-derived GBM xenografts and pre-miR-486-5p expression was measured using qRT-PCR 3 days after transfection. Nanoparticle-based delivery of miR-486-5p sponge decreased levels of endogenous miR-486-5p by approximately 80% (**Fig. 6A**) and simultaneously

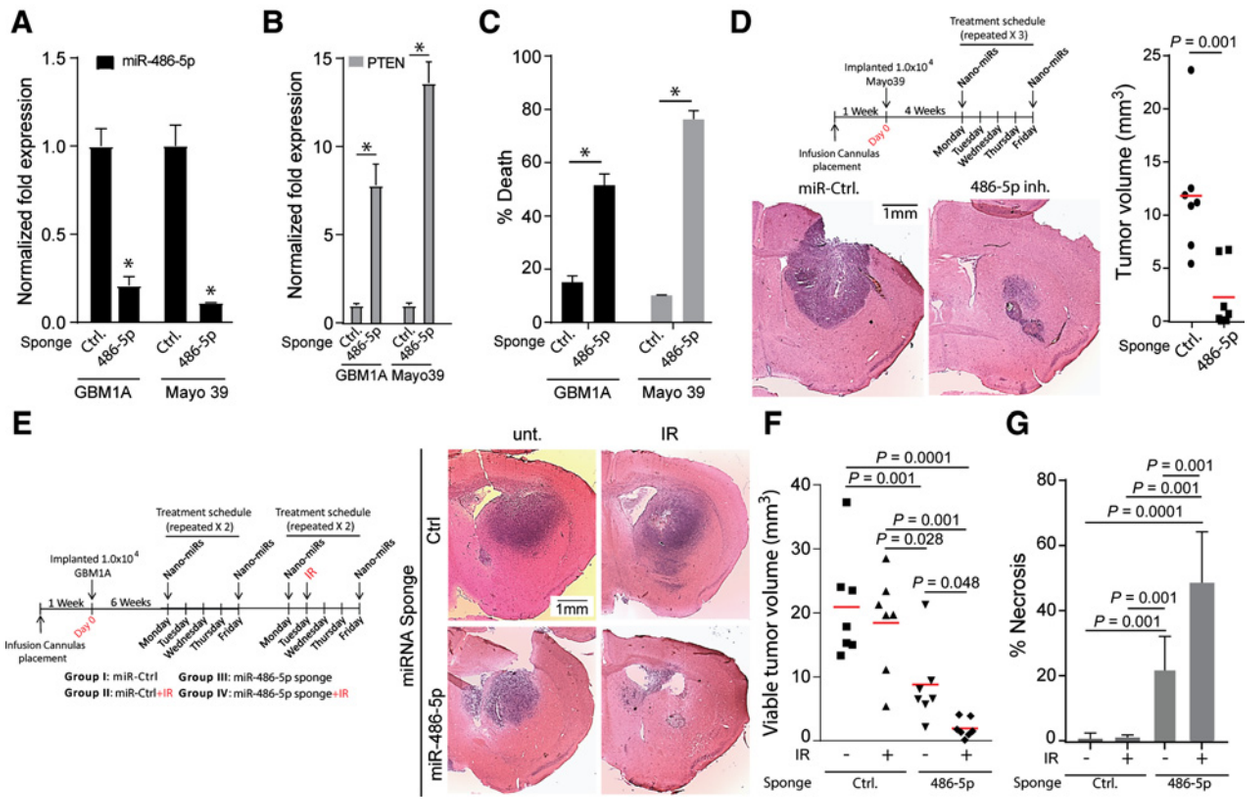

Figure 6.

In vivo inhibition of miR-486-5p in preestablished GBM reduces tumor size and sensitizes tumors to IR treatment. **A** and **B,** qRT-PCR analysis to quantify expression of miR-486-5p (**A**) or downstream target PTEN (**B**) in GBM1A and Mayo39 cells 3 days after transfection, with nano-miRs delivering a nontargeting control miRNA (Ctrl.) or a miR-486-5p sponge. **C,** Cell death assay to measure viability of GBM1A and Mayo 39 cells 6 days after transfections, with nano-miRs delivering a nontargeting control miRNA (Ctrl.) or a miR-486-5p sponge. **D,** Top, schematic summarizing treatment schedule for *in vivo* delivery of nano-miRs. Representative hematoxylin and eosin–stained brain sections from mice implanted with Mayo 39 cells ($n = 7$ for each group) treated with the indicated nano-miRs and then sacrificed 52 days after cell implantation. **E,** Schematic summarizing treatment schedule for *in vivo* delivery of nano-miRs and representative hematoxylin and eosin–stained brain sections (left) from mice implanted with GBM1A neurosphere cells ($n = 7$ for each group) treated with the indicated nano-miRs ± IR and then sacrificed 70 days after cell implantation. **F** and **G,** Maximum tumor cross-sectional areas of viable tumor tissue (**F**) or necrotic tissue (**G**) following treatment with nano-miRs quantified from hematoxylin and eosin–stained sections using ImageJ software. Student *t* test was used to calculate statistical significance in **A–D**; one-way ANOVA with Tukey *post hoc* test was used calculate statistical significance in **F** and **G**. Data are presented as means ± SD. *, $P < 0.05$.

significantly increased PTEN mRNA levels concurrent with a strong induction of cell death (**Fig. 6B** and **C**) recapitulating the results using the lentiviral system. These results show that miR-486-5p sponge retains biological activity and PTEN regulation when delivered to cells using PBAE nanoparticle complexes.

Mice bearing preestablished orthotopic patient-derived GBM xenografts (4 weeks post tumor cell implantation) were treated with nanoparticles containing either scrambled miRNA or miR-486-5p inhibitor by direct intratumoral infusion via a transcranial cannula twice per week for 3 weeks (**Fig. 6D**, top; ref. 15). Histopathologic examination of brains from animals sacrificed 3 days after the last nano-miR treatment (52 days post cell implantation) showed significantly smaller tumors in response to miR-486-5p antagomir delivery (**Fig. 6D**). Next, we asked whether *in vivo* miR-486-5p inhibition alters the therapeutic efficacy of ionizing radiation (IR), a standard-of-care treatment modality for GBM. For this purpose, GBM-derived neurospheres (GBM1A), which generate tumors that closely recapitulate the invasive growth pattern of clinical GBM (16), were implanted and beginning on postimplantation week 6 treated with nano-miRs as described above. A small number of animals were sacrificed prior to initiating therapies to confirm the presence of tumor (Supplementary Fig. S6). Two weeks after beginning nanoparticle infusions, a subset of animals began IR therapy in combination with either control or anti-miR-486-5p nano-miRs (see **Fig. 6E**, left for treatment schedule). Tumor burden and necrosis were quantified in brains collected 28 days after treatment initiation. Radiation alone had no statistically significant effects on tumor size or tumor-associated necrosis (**Fig. 6E–G**). Tumor size was significantly decreased in response to the active miRNA sponge and the most profound effects occurred in animals treated with miR-486-5p sponge + IR (**Fig. 6E** and **F**). The decrease in tumor size was accompanied by an increase in tumor tissue necrosis as measured by histopathology (**Fig. 6G**). These results show that combining *in vivo* inhibition of miR-486-5p with IR generated a cooperative antitumor response.

Discussion

miRNAs are short noncoding RNAs that control a wide range of biological processes including cell survival, oncogenesis, and cell stemness (23). We now understand that miRNAs can function as potent drivers of tumorigenesis and substantial efforts have been devoted to understanding how they are regulated and their downstream effectors to develop efficient ways to replenish tumor suppressor miRNAs and/or inhibit oncomiRs (24). Our results show that Oct4/Sox2 coexpression activates a network of miRNAs that correlate with the stem-like phenotype of GBM cells and predicts that they have oncogenic functions in GBM. In fact, miR-23b is thought to exert oncogenic functions in some cellular contexts by controlling cancer cell metabolism and autophagy (25). miR-10b-5p has been shown to function as an onco-miR in multiple settings and *ex vivo* inhibition can repress tumor-initiation capacity (26). miR-138 is dysregulated in multiple cancers and has been found to control many target genes related to proliferation, apoptosis, invasion, and migration (27). Recently, miR-222 has been implicated in controlling pathways that enhance survival of cancer cells to cytotoxic agents (28). However, how these miRNAs regulate the gene networks and phenotypes downstream of Oct4 and Sox2 remains to be elucidated.

miR-486-5p can activate or repress oncogenic pathways in a cell-type–specific manner acting as a tumor suppressor in esophageal, colorectal, lung, and liver cancers (29–32) while behaving as an oncomiR in pancreatic, brain, prostate, and hematopoietic tumors (33–37). We show that miR-486-5p expression associates with gain of stem cell phenotype in GBM neurospheres (**Fig. 1**) and is enriched in primary neurosphere isolates compared with glial progenitors (**Fig. 4C**), conditions where Sox2 is upregulated (13). Using bioinformatics analysis followed by ChIP-PCR, we validated Sox2-binding sites in the miR-486-5p putative promoter and we establish that Sox2 can directly transactivate miR-486-5p expression in GBM neurospheres using a combination of loss/gain-of-function approach and luciferase reporters (**Fig. 2**). We also demonstrate that transgenic miR-486-5p enhances GBM neurosphere resistance to IR treatment (**Fig. 4**) and self-renewal capacity of multiple GBM neurosphere isolates (**Fig. 1**). Our novel findings in GBM parallel studies showing that miR-486-5p expression is increased in leukemia compared with normal erythroid progenitor cells and transgenic expression enhances self-renewal, growth, survival, and drug sensitivity of CML progenitors (33, 35). Interestingly, and similar to results in the leukemia models (33), we did not observe a significant change in expression of well-characterized reprogramming transcription factors, stem cell markers, or lineage-specific markers in response to forced miR-486-5p expression. Our results demonstrate that miR-486-5p is a Sox2-regulated oncomiR in GBM neurospheres and suggest that the increase in self-renewal capacity observed in response to transgenic miR-486-5p is not directly related to dedifferentiating events but instead related to dysregulation of cell growth and survival mechanisms.

One oncogenic pathway that controls cell growth mechanisms and appears to be commonly affected by SOX2 alterations is the AKT pathway (38, 39). AKT activity is controlled by PTEN and cells that carry inactivating mutations in *PTEN* genes that exhibit constitutively active PI3K:AKT signaling, leading to inactivation of FoxO function though a mechanism involving phosphorylation-dependent nuclear exclusion (40). The PTEN:AKT:FoxO axis controls several cellular functions including cell growth, survival, and stemness (22, 41, 42). Interestingly, it has been speculated that miRNA dysregulation plays a significant role in PTEN transcriptional inhibition in gliomas (23). A recent report shows that miR-486-5p drives prostate cancer tumorigenesis by repressing PTEN and FoxO1 (36). Using GBM neurospheres expressing transgenic SOX2, conditions that activate miR-486-5p expression, we also identified PTEN and FoxO1 as miR-486-5p targets (**Fig. 3**). Furthermore, we show that forced SOX2 or miR-486-5p expression inhibits PTEN and FoxO1 mRNA and protein in addition to increasing AKT phosphorylation (**Fig. 3**; Supplementary Fig. S2). Interestingly, we show that PTEN, but not FoxO1 knockdown, is sufficient to abolish the effects of miR-486-5p inhibition (**Fig. 5F** and **G**), showing that PTEN is the predominant target responsible for miR-486-5p effects. These results demonstrate the novel findings that SOX2 activates oncogenic signals in GBM, at least in part, by repressing tumor suppressor genes and provides a new mechanism for AKT dysregulation in GBM neurospheres. Interestingly, while TCGA datasets show elevated levels of miR-486-5p GBM compared with nontumor tissue (**Fig. 4**), high miR-486-5p levels did not correlate with patient survival when considering all GBM cases (Supplementary Fig. S7). However, high levels of miR-486-5p and low levels of the miR-486-5p target PTEN and Bim were each found to correlate with worse outcome in patients with proneural GBM (Supplementary Fig. S7), a subtype characterized by increased Sox2 levels. Interestingly, despite observing an increase in *SOX2* gene expression in proneural GBM in the datasets analyzed, we did not observe a significant difference in patient survival between high and low expressers. This may be due to the relative low number of patients

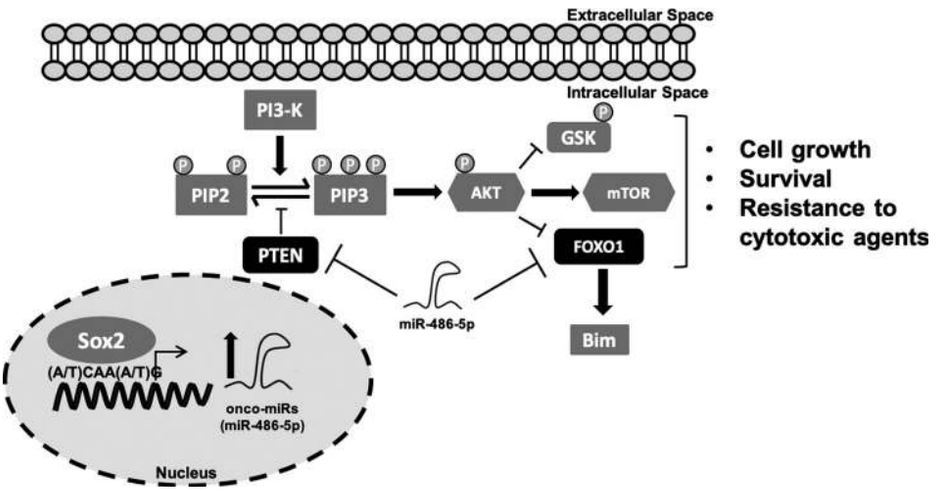

Figure 7.
Sox2 directly binds to the miR-486-5p promoter to activate expression in GBM neurospheres. miR-486-5p regulates expression of PTEN and FoxO1 by directly binding to their respective 3′UTRs and controlling mRNA levels. miR-486-5p activation indirectly contributes to AKT and Bim dysregulation, resulting in enhanced cell growth and GBM neurosphere resistance to IR.

analyzed, resulting in lack of power to achieve statistically significant differences (Supplementary Fig. S7).

One of the hallmarks of tumor suppressor gene inactivation is inhibition of cell death mechanisms and identifying ways to restore these mechanisms is a promising strategy to treat tumors (22, 43). High levels of SOX2 have been shown to inhibit apoptosis and reduce the effects of cancer therapeutics (5); however, the exact molecular mechanism involved in controlling this phenotype has been obscure. We show that forced expression of SOX2 represses tumor suppressor genes *PTEN* and *FoxO1*, two well-established regulators of apoptosis (19, 22), and identified miR-486-5p as a bona fide SOX2-regulated oncomiRs. In addition, we demonstrate that miR-486-5p inhibition strongly induces apoptosis through activation of proapoptotic BH3-only protein Bim (**Fig. 5**) concurrent with upregulation of PTEN (**Fig. 3G** and **H**). Bim is a downstream effector of PTEN that has been implicated in regulation of cell death mechanisms in cancer stem cells and resistance to GBM therapeutics (44). Also, forced expression of miR-486-5p made GBM neurosphere more resistant to IR (**Fig. 4**). Consistent with our observations that miR-486-5p acts as a critical determinant of GBM cell survival are reports showing that exosomes enriched with miR-486-5p inhibit apoptosis and reduce ischemic kidney injury by reducing PTEN expression and activating AKT signaling (45). Interestingly, a recent report shows that miR-486-5p is highly enriched in exosomes isolated from patients with GBM and can be used as part of a 7 miRNA signature to diagnose GBM preoperatively (46). Also, miR-486-5p plays a key role in maintaining skeletal muscle size by inhibiting PTEN and FoxO1 and activating AKT signaling to promote survival of muscle cells and prevent muscle wasting (47), highlighting how SOX2 dysregulation alters essential physiologic pathways, leading to enhanced survival. Taken together, these results establish a mechanism in which Sox2 activates miR-486-5p, resulting in PTEN and Bim dysregulation that contributes to the resistance to ionizing radiation (**Fig. 7**).

Substantial efforts have been devoted to understanding the downstream effectors of reprogramming transcription factors (e.g., SOX2) in an attempt to better understand tumorigenic mechanisms and identify new therapeutic avenues to treat cancer (5). We recently developed self-assembling miRNA-containing polymeric nanoparticles (nano-miRs) that effectively deliver miRNA mimics to human GBM cells *in vitro* and efficiently distribute through established orthotopic human GBM xenografts (15). Reprogramming transcription factors modulate miRNA networks and we have recently shown that reconstituting miRNA combinations (i.e., miR-148a + miR-296-5p) can have cooperative/synergistic effects, leading to the long-term survival and actual cures in preestablished orthotopic GBM xenograft models (15). We expand upon these findings by delivering miR-486-5p antagomirs to preestablished GBM xenografts and show that *in vivo* miR-486-5p inhibition significantly reduced tumor growth in two different orthotopic GBM models and enhanced the effects of IR therapy (**Fig. 6**). Although our findings successfully translate the molecular pathway that we rigorously define *in vitro* to the more complex *in vivo* setting, they do not completely rule out a role for indirect effects due to the inherent promiscuous nature of miRNAs. In addition, important future directions of this research is to determine the optimal combinations of miRNAs to "normalize," through either reconstitution or inhibition, to have a meaningful impact on survival in preclinical models as either monotherapy or in combination with current standard-of-care radiation/chemotherapy aimed at producing durable responses by reducing the emergence of more aggressive tumors that commonly result from single-agent targeted therapeutics.

In conclusion, SOX2 is an important regulator of tumorigenesis and the cancer stem cell phenotype that controls a vast network of coding and noncoding genes (5, 48). Despite our growing understanding of the SOX2 targetome, the targets that specifically regulate the tumor-propagating stem-like phenotype, and the subset of regulated targets amenable to therapeutic intervention remain subject of intense investigation (5). Our current results support a novel mechanism where SOX2 coordinates oncogenic signals in GBM neurospheres by directly transactivating miR-486-5p, which targets tumor suppressor genes PTEN and FoxO1, leading to subsequent inhibition of Bim expression, resulting in enhanced cell growth and survival of GBM neurospheres (**Fig. 7**). Our results demonstrate that miR-486-5p inhibition can be developed as a way to enhance the effects of current GBM standard of care.

Disclosure of Potential Conflicts of Interest

J.J. Green has ownership interest (including patents) as an inventor on related patents owned by JHU. No potential conflicts of interest were disclosed by the other authors.

Authors' Contributions

Conception and design: H. Lopez-Bertoni, I.S. Kotchetkov, H. Guerrero-Cazares, A. Quiñones-Hinojosa, J. Laterra
Development of methodology: H. Lopez-Bertoni, B. Lal, J.J. Green

Acquisition of data (provided animals, acquired and managed patients, provided facilities, etc.): H. Lopez-Bertoni, I.S. Kotchetkov, N. Mihelson, B. Lal, Y. Rui, A. Quiñones-Hinojosa, J. Laterra
Analysis and interpretation of data (e.g., statistical analysis, biostatistics, computational analysis): H. Lopez-Bertoni, I.S. Kotchetkov, B. Lal, H. Ames, A. Quiñones-Hinojosa, J. Laterra
Writing, review, and/or revision of the manuscript: H. Lopez-Bertoni, I.S. Kotchetkov, H. Ames, H. Guerrero-Cazares, A. Quiñones-Hinojosa, J.J. Green, J. Laterra
Administrative, technical, or material support (i.e., reporting or organizing data, constructing databases): H. Guerrero-Cazares, J.J. Green
Study supervision: J. Laterra
Other (helped by performing experiments and generating/analyzing results): M. Lugo-Fagundo

Acknowledgments

The authors would like to thank the following organizations for financial support: NIH R25 research fellowship (to I.S. Kotchetkov), NSF Graduate Research Fellowship DGE-1232825 (to Y. Rui), the Bloomberg~Kimmel Institute for Cancer Immunotherapy (to J.J. Green), Microscopy Core Grant (S10 OD016374) and the United States NIH grants R01NS073611 (to J. Laterra), R01EB016721 (to J.J. Green), and R01CA195503 (to J.J. Green).

The costs of publication of this article were defrayed in part by the payment of page charges. This article must therefore be hereby marked *advertisement* in accordance with 18 U.S.C. Section 1734 solely to indicate this fact.

Received May 28, 2019; revised July 26, 2019; accepted February 13, 2020; published first February 24, 2020.

References

1. Suva ML, Rheinbay E, Gillespie SM, Patel AP, Wakimoto H, Rabkin SD, et al. Reconstructing and reprogramming the tumor-propagating potential of glioblastoma stem-like cells. Cell 2014;157:580–94.
2. Ostrom QT, Gittleman H, de Blank PM, Finlay JL, Gurney JG, McKean-Cowdin R, et al. American Brain Tumor Association adolescent and young adult primary brain and central nervous system tumors diagnosed in the United States in 2008–2012. Neuro-Oncol 2016;18:i1–i50.
3. Bao S, Wu Q, McLendon RE, Hao Y, Shi Q, Hjelmeland AB, et al. Glioma stem cells promote radioresistance by preferential activation of the DNA damage response. Nature 2006;444:756–60.
4. Lathia JD, Mack SC, Mulkearns-Hubert EE, Valentim CL, Rich JN. Cancer stem cells in glioblastoma. Genes Dev 2015;29:1203–17.
5. Weina K, Utikal J. SOX2 and cancer: current research and its implications in the clinic. Clin Transl Med 2014;3:19.
6. Sarkar A, Hochedlinger K. The sox family of transcription factors: versatile regulators of stem and progenitor cell fate. Cell Stem Cell 2013;12:15–30.
7. Julian LM, McDonald AC, Stanford WL. Direct reprogramming with SOX factors: masters of cell fate. Curr Opin Genet Dev 2017;46:24–36.
8. Annovazzi L, Mellai M, Caldera V, Valente G, Schiffer D. SOX2 expression and amplification in gliomas and glioma cell lines. Cancer Genomics Proteomics 2011;8:139–47.
9. Gangemi RM, Griffero F, Marubbi D, Perera M, Capra MC, Malatesta P, et al. SOX2 silencing in glioblastoma tumor-initiating cells causes stop of proliferation and loss of tumorigenicity. Stem Cells 2009;27:40–8.
10. Esquela-Kerscher A, Slack FJ. Oncomirs - microRNAs with a role in cancer. Nat Rev Cancer 2006;6:259–69.
11. Acanda de la Rocha AM, Lopez-Bertoni H, Guruceaga E, Gonzalez-Huarriz M, Martinez-Velez N, Xipell E, et al. Analysis of SOX2-regulated transcriptome in glioma stem cells. PLoS One 2016;11:e0163155.
12. Fang X, Yoon JG, Li L, Yu W, Shao J, Hua D, et al. The SOX2 response program in glioblastoma multiforme: an integrated ChIP-seq, expression microarray, and microRNA analysis. BMC Genomics 2011;12:11.
13. Lopez-Bertoni H, Lal B, Li A, Caplan M, Guerrero-Cazares H, Eberhart CG, et al. DNMT-dependent suppression of microRNA regulates the induction of GBM tumor-propagating phenotype by Oct4 and Sox2. Oncogene 2015;34:3994–4004.
14. Lopez-Bertoni H, Lal B, Michelson N, Guerrero-Cazares H, Quinones-Hinojosa A, Li Y, et al. Epigenetic modulation of a miR-296-5p:HMGA1 axis regulates Sox2 expression and glioblastoma stem cells. Oncogene 2016;35:4903–13.
15. Lopez-Bertoni H, Kozielski KL, Rui Y, Lal B, Vaughan H, Wilson DR, et al. Bioreducible polymeric nanoparticles containing multiplexed cancer stem cell regulating miRNAs inhibit glioblastoma growth and prolong survival. Nano Lett 2018;18:4086–94.
16. Galli R, Binda E, Orfanelli U, Cipelletti B, Gritti A, De Vitis S, et al. Isolation and characterization of tumorigenic, stem-like neural precursors from human glioblastoma. Cancer Res 2004;64:7011–21.
17. Pandita A, Aldape KD, Zadeh G, Guha A, James CD. Contrasting in vivo and in vitro fates of glioblastoma cell subpopulations with amplified EGFR. Genes Chromosomes Cancer 2004;39:29–36.
18. Bartel DP. MicroRNAs: genomics, biogenesis, mechanism, and function. Cell 2004;116:281–97.
19. Koul D. PTEN signaling pathways in glioblastoma. Cancer Biol Ther 2008;7:1321–5.
20. Kale J, Osterlund EJ, Andrews DW. BCL-2 family proteins: changing partners in the dance towards death. Cell Death Differ 2018;25:65–80.
21. Shukla S, Saxena S, Singh BK, Kakkar P. BH3-only protein BIM: an emerging target in chemotherapy. Eur J Cell Biol 2017;96:728–38.
22. Zhang X, Tang N, Hadden TJ, Rishi AK. Akt, FoxO and regulation of apoptosis. Biochim Biophys Acta 2011;1813:1978–86.
23. Ames H, Halushka MK, Rodriguez FJ. miRNA regulation in gliomas: usual suspects in glial tumorigenesis and evolving clinical applications. J Neuropathol Exp Neurol 2017;76:246–54.
24. Rupaimoole R, Slack FJ. MicroRNA therapeutics: towards a new era for the management of cancer and other diseases. Nat Rev Drug Discov 2017;16:203–22.
25. Donadelli M, Dando I, Fiorini C, Palmieri M. Regulation of miR-23b expression and its dual role on ROS production and tumour development. Cancer Lett 2014;349:107–13.
26. Sheedy P, Medarova Z. The fundamental role of miR-10b in metastatic cancer. Am J Cancer Res 2018;8:1674–88.
27. Sha HH, Wang DD, Chen D, Liu SW, Wang Z, Yan DL, et al. MiR-138: a promising therapeutic target for cancer. Tumour Biol 2017;39:1010428317697575.
28. Dai H, Xu LY, Qian Q, Zhu QW, Chen WX. MicroRNA-222 promotes drug resistance to doxorubicin in breast cancer via regulation of miR-222/bim pathway. Biosci Rep 2019;39. DOI: 10.1042/BSR20190650.
29. Lang B, Zhao S. miR-486 functions as a tumor suppressor in esophageal cancer by targeting CDK4/BCAS2. Oncol Rep 2018;39:71–80.
30. Liu C, Li M, Hu Y, Shi N, Yu H, Liu H, et al. miR-486-5p attenuates tumor growth and lymphangiogenesis by targeting neuropilin-2 in colorectal carcinoma. Onco Targets Ther 2016;9:2865–71.
31. Shao Y, Shen YQ, Li YL, Liang C, Zhang BJ, Lu SD, et al. Direct repression of the oncogene CDK4 by the tumor suppressor miR-486-5p in non-small cell lung cancer. Oncotarget 2016;7:34011–21.
32. Sun H, Cui C, Xiao F, Wang H, Xu J, Shi X, et al. miR-486 regulates metastasis and chemosensitivity in hepatocellular carcinoma by targeting CLDN10 and CITRON. Hepatol Res 2015;45:1312–22.
33. Wang LS, Li L, Li L, Chu S, Shiang KD, Li M, et al. MicroRNA-486 regulates normal erythropoiesis and enhances growth and modulates drug response in CML progenitors. Blood 2015;125:1302–13.
34. Song L, Lin C, Gong H, Wang C, Liu L, Wu J, et al. miR-486 sustains NF-kappaB activity by disrupting multiple NF-kappaB-negative feedback loops. Cell Res 2013;23:274–89.
35. Shaham L, Vendramini E, Ge Y, Goren Y, Birger Y, Tijssen MR, et al. MicroRNA-486-5p is an erythroid oncomiR of the myeloid leukemias of Down syndrome. Blood 2015;125:1292–301.
36. Yang Y, Ji C, Guo S, Su X, Zhao X, Zhang S, et al. The miR-486-5p plays a causative role in prostate cancer through negative regulation of multiple tumor suppressor pathways. Oncotarget 2017;8:72835–46.
37. Mees ST, Mardin WA, Sielker S, Willscher E, Senninger N, Schleicher C, et al. Involvement of CD40 targeting miR-224 and miR-486 on the progression of pancreatic ductal adenocarcinomas. Ann Surg Oncol 2009;16:2339–50.
38. Ren C, Ren T, Yang K, Wang S, Bao X, Zhang F, et al. Inhibition of SOX2 induces cell apoptosis and G1/S arrest in Ewing's sarcoma through the PI3K/Akt pathway. J Exp Clin Cancer Res 2016;35:44.

39. Li Y, Chen K, Li L, Li R, Zhang J, Ren W. Overexpression of SOX2 is involved in paclitaxel resistance of ovarian cancer via the PI3K/Akt pathway. Tumour Biol 2015;36:9823–8.
40. Song MS, Salmena L, Pandolfi PP. The functions and regulation of the PTEN tumour suppressor. Nat Rev Mol Cell Biol 2012;13:283–96.
41. Zhang X, Yalcin S, Lee DF, Yeh TY, Lee SM, Su J, et al. FOXO1 is an essential regulator of pluripotency in human embryonic stem cells. Nat Cell Biol 2011;13:1092–9.
42. Rivas S, Gomez-Oro C, Anton IM, Wandosell F. Role of Akt isoforms controlling cancer stem cell survival, phenotype and self-renewal. Biomedicines 2018;6. DOI: 10.3390/biomedicines6010029.
43. Ma DD, Yang WX. Engineered nanoparticles induce cell apoptosis: potential for cancer therapy. Oncotarget 2016;7:40882–903.
44. Aroui S, Dardevet L, Najlaoui F, Kammoun M, Laajimi A, Fetoui H, et al. PTEN-regulated AKT/FoxO3a/Bim signaling contributes to Human cell glioblastoma apoptosis by platinum-maurocalcin conjugate. Int J Biochem Cell Biol 2016;77:15–22.
45. Vinas JL, Burger D, Zimpelmann J, Haneef R, Knoll W, Campbell P, et al. Transfer of microRNA-486-5p from human endothelial colony forming cell-derived exosomes reduces ischemic kidney injury. Kidney Int 2016;90:1238–50.
46. Ebrahimkhani S, Vafaee F, Hallal S, Wei H, Lee M, Young P, et al. Deep sequencing of circulating exosomal microRNA allows non-invasive glioblastoma diagnosis. NPJ Precis Oncol 2018;2:28.
47. Alexander MS, Casar JC, Motohashi N, Vieira NM, Eisenberg I, Marshall JL, et al. MicroRNA-486-dependent modulation of DOCK3/PTEN/AKT signaling pathways improves muscular dystrophy-associated symptoms. J Clin Invest 2014;124:2651–67.
48. Song WS, Yang YP, Huang CS, Lu KH, Liu WH, Wu WW, et al. Sox2, a stemness gene, regulates tumor-initiating and drug-resistant properties in CD133-positive glioblastoma stem cells. J Chin Med Assoc 2016;79:538–45.